Collapse of the Normal-State Pseudogap at a Lifshitz Transition in the $Bi_2Sr_2CaCu_2O_{8+\delta}$ Cuprate Superconductor

S. Benhabib,[1] A. Sacuto,[1,*] M. Civelli,[2] I. Paul,[1] M. Cazayous,[1] Y. Gallais,[1] M.-A. Méasson,[1] R. D. Zhong,[3] J. Schneeloch,[3] G. D. Gu,[3] D. Colson,[4] and A. Forget[4]

[1]*Laboratoire Matériaux et Phénomènes Quantiques (UMR 7162 CNRS), Université Paris Diderot-Paris 7, Bâtiment Condorcet, 75205 Paris Cedex 13, France*

[2]*Laboratoire de Physique des Solides, UMR 8502 CNRS, Université Paris Sud, Bâtiment 510, 91405 Orsay Cedex, France*

[3]*Matter Physics and Materials Science, Brookhaven National Laboratory (BNL), Upton, New York 11973, USA*

[4]*Service de Physique de l'Etat Condensé, CEA-Saclay, 91191 Gif-sur-Yvette, France*

(Received 21 October 2014; published 7 April 2015)

We report a fine tuned doping study of strongly overdoped $Bi_2Sr_2CaCu_2O_{8+\delta}$ single crystals using electronic Raman scattering. Combined with theoretical calculations, we show that the doping, at which the normal-state pseudogap closes, coincides with a Lifshitz quantum phase transition where the active holelike Fermi surface becomes electronlike. This conclusion suggests that the microscopic cause of the pseudogap is sensitive to the Fermi surface topology. Furthermore, we find that the superconducting transition temperature is unaffected by this transition, demonstrating that their origins are different on the overdoped side.

DOI: 10.1103/PhysRevLett.114.147001 PACS numbers: 74.72.Gh, 74.25.nd, 74.62.Dh, 74.72.Kf

Revealed more than twenty-five years ago by nuclear magnetic resonance [1–3], the pseudogap phase in cuprates remains hitherto a mysterious state of matter out of which the high-temperature superconductivity emerges. The pseudogap appears below the T^* temperature and manifests itself as a loss of quasiparticle spectral weight. Although intensely studied in the underdoped regime [4–6], relatively less is known about the pseudogap on the overdoped side, where it weakens and eventually disappears. Thus, a logical line of enquiry is to study the pseudogap closing as a function of doping p, and to identify what triggers it in the first place.

In systems where $T^*(p)$ intersects the superconducting dome described by the critical temperature $T_c(p)$, this task is complicated by the appearance of the superconducting phase. One way to proceed is to perform such a study at the lowest available temperatures, either in the superconducting phase [7–12], or by suppressing it with a magnetic field [13] or disorder [14]. Often such studies have inferred a quantum phase transition [15–17] associated with the pseudogap closing.

A second possibility is to track the *normal-state* pseudogap at a higher temperature, and to study the vicinity of the doping p_c where it closes. Since p_c, defined as the doping where $T^*(p) = T_c(p)$, is essentially a finite temperature property, *a priori* it is not clear if it is linked to a quantum phase transition.

In this work our main result is to show that in $Bi_2Sr_2CaCu_2O_{8+\delta}$ (Bi-2212) p_c is indeed tied to a Lifshitz quantum phase transition where the underlying holelike active Fermi surface becomes electronlike at a van Hove singularity. Interestingly, we find that T_c is unaffected by this transition. Moreover, comparing our results with existing photoemission and tunnelling data of several hole-doped cuprates, we infer that the microscopic origins of the pseudogap and the superconductivity are generically different on the overdoped side. Only the former is tied to the change in the Fermi surface topology, which removes quasiparticles from regions in momentum space of high scattering rate (hot regions). While the collapse of the normal-state pseudogap [18–20], as well as the change of Fermi surface topology [21] have been reported, to the best of our knowledge, the link between the two has not been demonstrated before in Bi-2212. Consequently, our result provides an important clue regarding the microscopic origin of the normal-state pseudogap, and its relation with superconductivity.

One technical obstacle to studying the closing of the pseudogap is the lack of sufficiently overdoped samples belonging to the same family of cuprates. Indeed, our study was made possible due to the availability of several high quality Bi-2212 single crystals with doping close to p_c, as reported in the Supplemental Material [22]. The level of doping was controlled only by oxygen insertion, and the highest doping achieved was around $p = 0.24$. This allowed us to perform a careful finely tuned electronic Raman study of the doping dependence and determine $p_c = 0.22$.

The Raman measurements were performed in $\nu = B_{1g}, B_{2g}$ geometries that probe, respectively, the antinodal (AN) region near $(\pm\pi, 0)$ and $(0, \pm\pi)$ and the nodal (N) region near $(\pm\pi/2, \pm\pi/2)$, (cf. Ref. [22]). Our spectra are comparable with earlier studies with a different laser line [23,24], thereby demonstrating the absence of resonance effects in the overall conclusions. In the following, the quantity of importance is the integrated Raman intensity defined by

$$I_\nu(T) = \int_0^\Lambda d\omega \chi''_\nu(\omega, T), \tag{1}$$

extracted from the Raman response $\chi''_\nu(\omega, T)$ where Λ is a cutoff. We experimentally demonstrate our main result in two steps.

In the first step we determine p_c precisely, which is a refinement of our earlier work [18]. In Figs. 1(a)–1(d), we report Raman responses $\chi''_{B_{1g}}(\omega, T)$ at different temperatures and for different overdoped (OD) compounds. The temperature dependences of the corresponding integrated intensities $I_{B_{1g}}(T)$ are shown in Figs. 1(e)–1(h). In Fig. 1(a), we show the spectra for the Bi-2212 OD80 compound. We observe that the pair-breaking peak ($2\Delta_0$), located at 408 cm^{-1}, decreases in intensity with increasing temperature and disappears at T_c. Correspondingly, $I_{B_{1g}}(T)$ decreases monotonically exhibiting a dip at T_c [Fig. 1(e)]. Just above T_c, however, the low energy spectral weight (below 408 cm^{-1}) increases (positive slope) with temperature.

This recovery of spectral weight,which can be as large as 15% for $p = 0.11$ (cf. Fig. 3 in the Supplemental Material [22]), is the signature of the presence of the pseudogap in the normal-state spectra. Note that, this T dependence is opposite to that of a normal metal. Therefore, above T_c, $I_{B_{1g}}(T)$ increases monotonically, until it reaches a maximum at a temperature T^* that defines the onset temperature of the pseudogap [Fig. 1(e)]. Above T^*, the T dependence of $I_{B_{1g}}$ is the one of a normal metal. Our estimate of $T^*(p)$ is in good agreement with previous transport and spectroscopy measurements (cf. Fig. 4 of the Supplemental Material [22]). As the doping level increases [Figs. 1(a)–1(d)], the difference between T_c and T^* shrinks, and disappears at $p_c = 0.22$, indicating the collapse of the normal-state pseudogap. For $p > 0.22$ the slope of $I_{B_{1g}}(T)$ just above T_c is negative, implying there is no signature of the normal-state pseudogap anymore. Quantitatively, this behavior is captured by the doping dependence of the loss of the spectral intensity, defined by $I_{B_{1g}}(T_c) - I_{B_{1g}}(T^*)$ and which we report in Fig. 3 as black stars. Note that a change in the slope of $I_{B_{1g}}(T)$ at $p \geq 0.22$ appears at $T \approx 100$ K which is definitely higher than the pseudogap $T^* \approx 60$ K. Consequently, this feature is not related to the pseudogap, and its origin is currently under investigation.

The second step involves comparing the spectra in the B_{1g} and B_{2g} geometries, and following their doping evolutions around p_c at fixed temperatures. Importantly, we succeeded in measuring the B_{1g} and B_{2g} Raman responses of each crystal on the same laser spot (see Ref. [22]). We first show in Fig. 2 representative $\chi''_{B_{1g}}(\omega)$ [red (grey)] and $\chi''_{B_{2g}}(\omega)$ (black) Raman responses, at 10 K (superconducting state) and at 110 K (normal state) for selected doping levels. The Raman shift is expressed in units of the superconducting gap $\Delta_0(p)$, in order to compare better samples with varying gap values. Note that, both in the superconducting and the normal states, the B_{1g} response increases continuously in magnitude compared to the B_{2g} response for $p \leq 0.22$, consistent with earlier

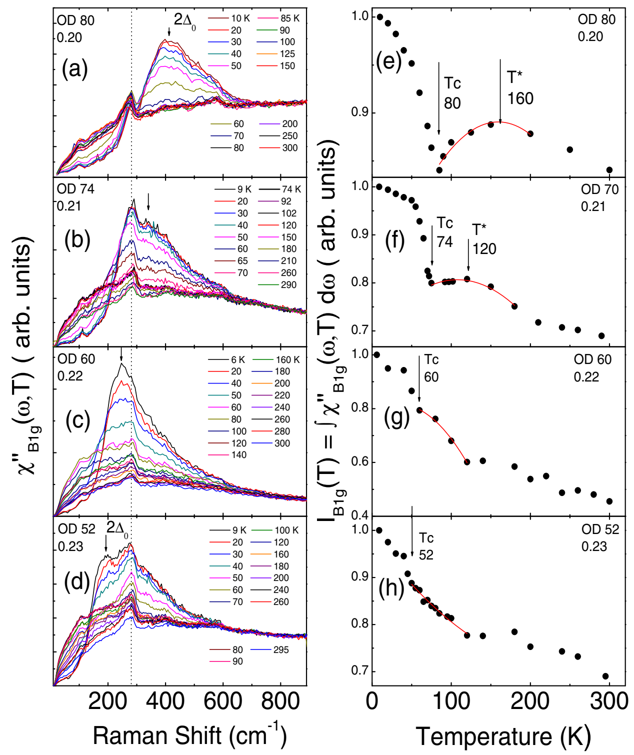

FIG. 1 (color online). (a)–(d) T dependence of the Raman response $\chi''_{B_{1g}}$ of overdoped Bi-2212. $2\Delta_0$ is defined as the position of the B_{1g} pair breaking peak. The location of the 300 cm^{-1} phonon peak is marked by a dotted line. (e)–(h) Integrated Raman intensities are shown in (a)–(d), with cutoff $\Lambda = 850$ cm^{-1}. For each doping, $I_{B_{1g}}(T)$ is normalized by $I_{B_{1g}}$ (10 K). The red curve is a second order polynomial fit just above T_c indicating the sign change of the slope. We found a remarkably linear dependence between T_c and $2\Delta_0$ in the critical temperature range 90–50 K (cf. Ref. [22]). The doping level for each value of T_c was fixed using the Tallon-Presland formula (cf. Ref. [22]).

studies [23,25–31]. However, the crucial finding of the current work is that this trend changes and the B_{1g} response starts to decrease beyond 0.22 doping.

The above nonmonotonic doping dependence is best quantified by extracting the ratio of the integrated intensities $I_{B_{1g}}/I_{B_{2g}}$ from the Raman responses $\chi''_\nu(\omega)$ using Eq. (1). Studying the intensity ratio, rather than the absolute intensities, allows us to avoid spurious effects due to nonintrinsic intensity modulations that may occur when passing from one crystal to another (cf. Ref. [22]). Note that, in principle $I_{B_{1g}}$ contains not only the contribution of the electronic background (which is what we are interested in), but also that of the phonon peaked sharply at 300 cm^{-1} (see the dotted line in Fig. 1). However, by comparing the current spectra with that obtained using a 647.1 nm laser line, in which the phonon peak is absent, we are able to confirm that $I_{B_{1g}}$, and especially its doping dependence, is mostly due to the electronic background [32].

In Fig. 3 we report the doping dependencies of the intensity ratios $I_{B_{1g}}/I_{B_{2g}}$ in the superconducting (filled

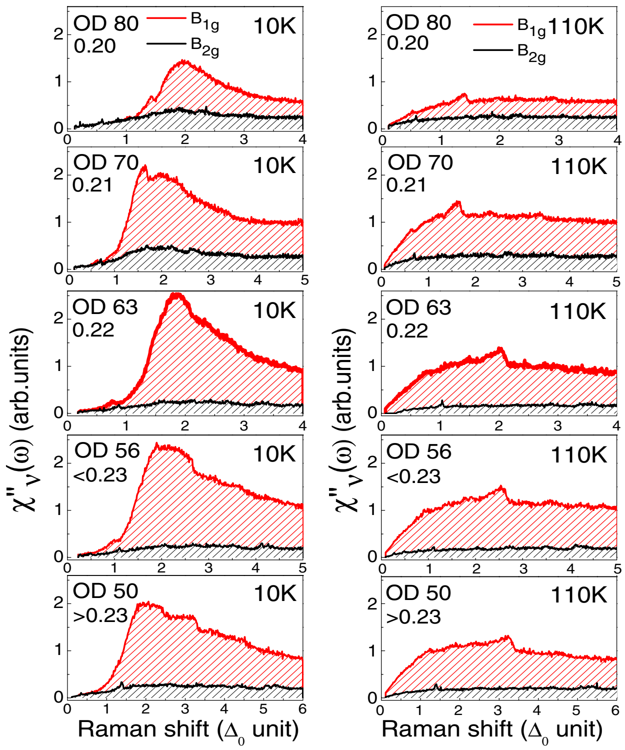

FIG. 2 (color online). B_{1g} (red/grey) and B_{2g} (black) Raman responses of Bi-2212 at 10 K (superconducting state) and 110 K (normal state) in the overdoped range using a 532 nm laser. The [red (grey)] and black hatched areas indicate the magnitudes of the B_{1g} and the B_{2g} responses, respectively. The former increases compared to the latter as a function of doping up to $p_c = 0.22$.

circles) and the normal states (open circles). Note that, the ratios in the two phases are nearly the same, thereby indicating that $I_{B_{1g}}/I_{B_{2g}}$ is unaffected by the superconducting gap. Most importantly, the ratios change nonmonotonically as a function of p, and they reveal a sharp peak located at $p_c = 0.22$, the doping where the normal-state pseudogap closes (black stars). We confirmed that the sharp peak is not a resonance effect, since it is visible with two distinct laser lines (532 nm and 647.1 nm).

Note that the peak in $I_{B_{1g}}/I_{B_{2g}}$ cannot be attributed to the doping dependence of the pseudogap which is monotonic. Instead, the temperature independence of the sharp peak position indicates that it is related to enhanced density of states of the underlying band structure around the AN region of the Brillouin zone. This invariably leads to the possibility of a doping induced Lifshitz transition wherein, as a van Hove singularity crosses the chemical potential, the open holelike antibonding Fermi surface closes around the $(\pm\pi, 0)$ and $(0, \pm\pi)$ points and becomes electronlike. An electronlike antibonding band in Bi-2212 at $p > 0.22$ has been reported by ARPES data [21], but this change of topology was not linked with the closing of the pseudogap.

In order to support this scenario we perform a theoretical calculation of the Raman response function using a minimal tight-binding model with the normal-state dispersion [33]: $\epsilon_{k,\alpha} = -2t(\cos k_x + \cos k_y) + 4t' \cos k_x \cos k_y \pm t_o(\cos k_x - \cos k_y)^2/4 - \mu$. Here $\alpha = \pm$ refer to the antibonding (AB) and the bonding (B) bands. The superconducting dispersion is $E_k = \sqrt{\epsilon_k^2 + \Delta_k^2}$, with $\Delta_k = \Delta_0(\cos k_x - \cos k_y)/2$. We take $t' = -0.3t$, $t_o = 0.084t$, and a doping independent $\Delta_0 = 0.0025t$. We change p by varying the chemical potential μ. As shown in Figs. 4(a)–4(c), this model undergoes a Lifshitz transition at $p_c = 0.22$ where the AB band changes from being holelike to electronlike (the B band remains holelike in this doping range, see the Supplemental Material [22]). For simplicity we take a constant electron scattering rate $\Gamma_N = 0.01t$ and $\Gamma_S = 0.0025t$ in the normal and the superconducting states, respectively. An earlier work has shown that the scattering rates measured from the slopes of the Raman responses become isotropic around $p \approx 0.22$ [23]. The calculation of $\chi''_\nu(\omega)$ and I_ν are standard (for details, cf. Ref. [22]). The doping dependence of the calculated ratio $I_{B_{1g}}/I_{B_{2g}}$ shows prominent peaks at $p = 0.22$ [see Fig. 4(d)], both in the normal and the superconducting states, and reproduces qualitatively the experimental trend of Fig. 3.

The origin of the peak can be captured conveniently by tracking the doping dependence of the Raman vertex $\gamma^\nu_{k,\alpha}$-weighted density of states $N_\nu(\omega) \equiv \sum_{k,\alpha}(\gamma^\nu_{k,\alpha})^2\delta(\omega - \epsilon_{k,\alpha})$ which enter the calculation of I_ν. As shown in

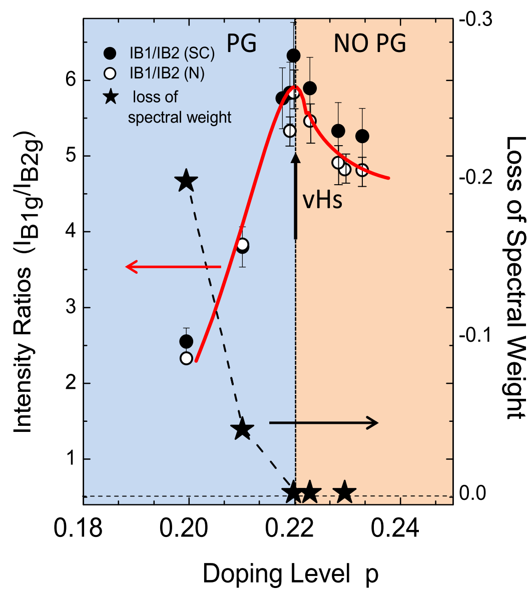

FIG. 3 (color online). Doping evolution of (i) the ratio $I_{B_{1g}}/I_{B_{2g}}$ of the integrated intensity [defined in Eq. (1)] in the superconducting and the normal states (filled and open circles respectively) with cutoff $\Lambda \approx 3\Delta_0$, (ii) the loss of spectral weight related to the pseudogap (black stars). The peak in the ratio $I_{B_{1g}}/I_{B_{2g}}$, both for the superconducting and the normal phases, coincides with the critical doping $p_c = 0.22$ where the pseudogap disappears. The peak is a consequence of a Lifshitz transition where the holelike Fermi surface of the dominant antibonding band becomes electronlike as the chemical potential crosses a van Hove singularity.

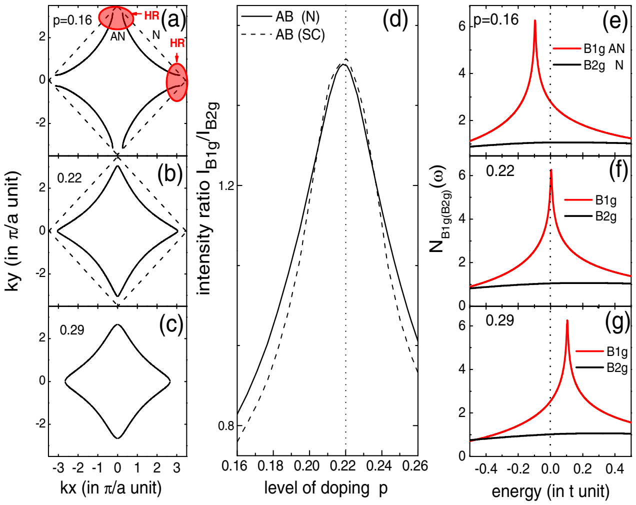

FIG. 4 (color online). (a)–(c) With doping, the holelike antibonding Fermi surface becomes electronlike at a Lifshitz transition. The dotted line is the antiferromagnetic Brillouin zone. HR denotes the hot region of the large scattering rate. (d) Doping dependence of the integrated intensity ratio $I_{B_{1g}}/I_{B_{2g}}$ in the normal (solid line) and superconducting (dashed line) states calculated from a theoretical model (see text), reproducing qualitatively the trend of Fig. 3. The curves are normalized (cf. Ref. [22]). (e)–(g) The associated van Hove singularity appears in $N_{B_{1g}}(\omega)$ (red/grey), the density of states weighted by the B_{1g} Raman vertex (defined in text). The van Hove singularity does not however appear in $N_{B_{2g}}(\omega)$ (black),which is multiplied by $(t/t')^2$ for better visibility.

Figs. 4(e)–4(g), the van Hove singularity shows up in $N_{B_{1g}}(\omega)$, and the peak in the intensity $I_{B_{1g}}$ corresponds to the van Hove singularity crossing the chemical potential. Simultaneously, since the B_{2g} geometry probes the diagonal directions of the Brillouin zone, $N_{B_{2g}}(\omega)$ is unaffected by the van Hove singularity and therefore $I_{B_{2g}}$ has no significant doping dependence.

Based on the Mott formula, at the Lifshitz transition $p = 0.22$ we expect a change in the sign of the Seebeck coefficient, provided the scattering rates are isotropic [34]. However, as noted in an earlier work [21], the Hall coefficient may remain positive across the Lifshitz transition, as observed in thin film studies [35].

A possible interpretation of our results is that the Lifshitz transition avoids the pseudogap by effectively moving quasiparticles from regions of strong scattering (hot regions) located around $(\pm\pi, 0)$ and $(0, \pm\pi)$ [see panels (a)–(c), Fig. 4]. Note that, this possibility is independent of the origin of the hot regions which could arise from fluctuations of antiferromagnetic spin waves [36–39] or charge-density waves (related to long-ranged incommensurate charge modulations) [40–45], or from Mott-related physics [46–50]. A second quantum critical point at $p*$ inside the superconducting dome, separating a small from a large Fermi surface phase, has been inferred, for example, in recent scanning tunnelling microscopy [10,11] and ARPES [20] experiments.

An intriguing pattern emerges upon comparing our results with those on other hole doped cuprate families near p_c. In contrast with Bi-2212 and $La_{1.6-x}Nd_{0.4}Sr_xCuO_4$ [13] where p_c is located well inside the superconducting dome, in the ARPES measurements on $La_{2-x}Sr_xCuO_4$ (LSCO) of Ref. [51] the endpoints of the pseudogap and the superconducting phases are nearby in doping. Scanning tunneling spectroscopy on $Bi_2Sr_2CuO_{6+\delta}$,(Bi-2201) instead, found the pseudogap extending well into the normal phase [52]. This suggests that the position of p_c with respect to the superconducting dome is material dependent (see Fig. 5). Interestingly, just as we established here for Bi-2212, for both LSCO and Bi-2201 data analyses have suggested the coincidence of the pseudogap closing with a Lifshitz transition [51,52]. Taken together, this appears to be a universal feature of the hole doped cuprates, and our findings establish an intimate connection between the normal-state pseudogap and Fermi surface topology. In $Tl_2Ba_2CuO_{6+\delta}$ (Tl-2201) the scenario is less clear, as the observation of the pseudogap is still debated [53].

Few studies [16,54] on Bi-2212 and $YBa_2Cu_3O_{7-x}$,(Y-123) have reported the pseudogap closing at $p = 0.19$. This might simply imply that the normal state and the superconducting pseudogaps close at different dopings [20]. Alternatively, this apparent discrepancy could be related to the fact that in-plane transport and superfluid density are mostly sensitive to the nodal properties [38], while c-axis transport and the B_{1g} Raman response probe mostly the antinodal properties [55]. Next, in our scenario it is possible that for $p > 0.22$ the pseudogap exists in the holelike B band, but we do not find any signature of it in the Raman spectra, consistent with ARPES results [20]. One possibility is that the response is predominantly from the AB band since it is close to a density of states singularity. We notice this trend in the theoretical calculation as well (cf. Ref. [22]).

In conclusion, our results demonstrate that the mechanism that gives rise to the normal-state pseudogap is sensitive to the topology of the Fermi surface, and is operational only when the latter is holelike. Furthermore,

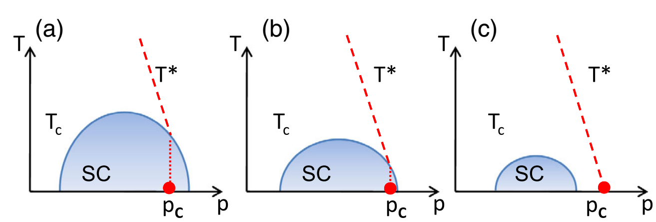

FIG. 5 (color online). Schematic phase diagram of temperature (T) versus doping (p) with with three material-dependent possible locations of the critical doping p_c. This latter is defined where the normal state pseudogap closes, with respect to the superconducting (SC) dome [shaded blue (grey)]. (a) is realized in Bi-2212 (current study), (b) and (c) have been reported for LSCO [51] and Bi-2201 [52], respectively. The common feature in all three cases is the coincidence of p_c with a Lifshitz transition where a Fermi surface changes from holelike to electronlike.

we conclude that, on the overdoped side of the cuprates, the microscopic origins of the pseudogap and the superconductivity are different.

We are grateful to A. Georges, J. Tallon, A. Chubukov, M. Norman, L. Taillefer, C. Pépin, Ph. Bourges, Y. Sidis, A. Damascelli, and H. Alloul for very helpful discussions.

*alain.sacuto@univ-paris-diderot.fr

[1] H. Alloul, T. Ohno, and P. Mendels, Phys. Rev. Lett. **63**, 1700 (1989).
[2] W. W. Warren, R. E. Walstedt, G. F. Brennert, R. J. Cava, R. Tycko, R. F. Bell, and G. Dabbagh, Phys. Rev. Lett. **62**, 1193 (1989).
[3] T. Imai, H. Yasuoka, T. Shimizu, Y. Ueda, K. Yoshimura, and K. Kosuge, Physica (Amsterdam) **162C–164C**, Part 1, 169 (1989).
[4] T. Timusk and B. Statt, Rep. Prog. Phys. **62**, 61 (1999).
[5] M. R. Norman, D. Pines, and C. Kallin, Adv. Phys. **54**, 715 (2005).
[6] L. Taillefer, Annu. Rev. Condens. Matter Phys. **1**, 51 (2010).
[7] J. Loram, J. Luo, J. Cooper, W. Liang, and J. Tallon, J. Phys. Chem. Solids **62**, 59 (2001).
[8] A. Shekhter, B. J. Ramshaw, R. Liang, W. N. Hardy, D. A. Bonn, F. F. Balakirev, R. D. McDonald, J. B. Betts, S. C. Riggs, and A. Migliori, Nature (London) **498**, 75 (2013).
[9] L. Mangin-Thro, Y. Sidis, P. Bourges, S. De Almeida-Didry, F. Giovannelli, and I. Laffez-Monot, Phys. Rev. B **89**, 094523 (2014).
[10] K. Fujita *et al.*, Science **344**, 612 (2014).
[11] Y. He *et al.*, Science **344**, 608 (2014).
[12] Y. H. Liu, Y. Toda, K. Shimatake, N. Momono, M. Oda, and M. Ido, Phys. Rev. Lett. **101**, 137003 (2008).
[13] R. Daou *et al.*, Nat. Phys. **5**, 31 (2009).
[14] H. Alloul, J. Bobroff, M. Gabay, and P. J. Hirschfeld, Rev. Mod. Phys. **81**, 45 (2009).
[15] C. M. Varma, Phys. Rev. Lett. **83**, 3538 (1999).
[16] J. Tallon and J. Loram, Physica (Amsterdam) **349C**, 53 (2001).
[17] S. Sachdev, Physica (Amsterdam) **470C**, Suppl. 1, S4 (2010).
[18] A. Sacuto, Y. Gallais, M. Cazayous, M.-A. Méasson, G. D. Gu, and D. Colson, Rep. Prog. Phys. **76**, 022502 (2013).
[19] U. Chatterjee *et al.*, Proc. Natl. Acad. Sci. U.S.A. **108**, 9346 (2011).
[20] I. M. Vishik *et al.*, Proc. Natl. Acad. Sci. U.S.A. **109**, 18332 (2012).
[21] A. Kaminski, S. Rosenkranz, H. M. Fretwell, M. R. Norman, M. Randeria, J. C. Campuzano, J.-M. Park, Z. Z. Li, and H. Raffy, Phys. Rev. B **73**, 174511 (2006).
[22] See Supplemental Material at http://link.aps.org/supplemental/10.1103/PhysRevLett.114.147001 for details of the Raman experiments,the crystal Growth and characterization, the estimate of Δ_0 and its relationship to T_c, details on the signature of the pseudogap, the comparison between T^* determined from Raman and c-axis transport and other spectroscopy probes and more details on the theoretical results
[23] F. Venturini, M. Opel, T. P. Devereaux, J. K. Freericks, I. Tütto, B. Revaz, E. Walker, H. Berger, L. Forró, and R. Hackl, Phys. Rev. Lett. **89**, 107003 (2002).
[24] F. Venturini, M. Opel, R. Hackl, H. Berger, L. Forró, and B. Revaz, J. of Phys. Chem. of Solids **63**, 2345 (2002).
[25] S. Blanc, Y. Gallais, A. Sacuto, M. Cazayous, M. A. Méasson, G. D. Gu, J. S. Wen, and Z. J. Xu, Phys. Rev. B **80**, 140502 (2009).
[26] K. C. Hewitt and J. C. Irwin, Phys. Rev. B **66**, 054516 (2002).
[27] N. Munnikes *et al.*, Phys. Rev. B **84**, 144523 (2011).
[28] T. Masui, M. Limonov, H. Uchiyama, S. Lee, S. Tajima, and A. Yamanaka, Phys. Rev. B **68**, 060506 (2003).
[29] T. Masui, T. Hiramachi, K. Nagasao, and S. Tajima, Phys. Rev. B **79**, 014511 (2009).
[30] J. G. Naeini, X. K. Chen, J. C. Irwin, M. Okuya, T. Kimura, and K. Kishio, Phys. Rev. B **59**, 9642 (1999).
[31] L. V. Gasparov, P. Lemmens, N. N. Kolesnikov, and G. Güntherodt, Phys. Rev. B **58**, 11753 (1998).
[32] The phonon peak contribution is less than 3% of the total integrated area.
[33] A. A. Kordyuk, S. V. Borisenko, M. Knupfer, and J. Fink, Phys. Rev. B **67**, 064504 (2003).
[34] J. M. Buhmann and M. Sigrist, Phys. Rev. B **88**, 115128 (2013).
[35] Z. Konstantinović, Z. Z. Li, and H. Raffy, Phys. Rev. B **62**, R11989 (2000).
[36] A. V. Chubukov, Europhys. Lett. **44**, 655 (1998).
[37] J. Schmalian, D. Pines, and B. Stojković, Phys. Rev. Lett. **80**, 3839 (1998).
[38] L. B. Ioffe and A. J. Millis, Phys. Rev. B **58**, 11631 (1998).
[39] S. Chakravarty, R. B. Laughlin, D. K. Morr, and C. Nayak, Phys. Rev. B **63**, 094503 (2001).
[40] Y. Wang and A. Chubukov, Phys. Rev. B **90**, 035149 (2014).
[41] R. Comin *et al.*, Science **343**, 390 (2014).
[42] E. H. da Silva Neto *et al.*, Science **343**, 393 (2014).
[43] T. Wu, H. Mayaffre, S. Krämer, M. Horvatić, C. Berthier, W. N. Hardy, R. Liang, D. A. Bonn, and M.-H. Julien, Nat. Commun. **6**, 6438 (2015).
[44] S. E. Sebastian, N. Harrison, F. F. Balakirev, M. M. Altarawneh, P. A. Goddard, R. Liang, D. A. Bonn, W. N. Hardy, and G. G. Lonzarich, Nature (London) **511**, 61 (2014).
[45] C. Pépin, V. S. de Carvalho, T. Kloss, and X. Montiel, Phys. Rev. B **90**, 195207 (2014).
[46] M. Civelli, M. Capone, S. S. Kancharla, O. Parcollet, and G. Kotliar, Phys. Rev. Lett. **95**, 106402 (2005).
[47] B. Kyung, S. S. Kancharla, D. Sénéchal, A.-M. S. Tremblay, M. Civelli, and G. Kotliar, Phys. Rev. B **73**, 165114 (2006).
[48] M. Ferrero, P. S. Cornaglia, L. De Leo, O. Parcollet, G. Kotliar, and A. Georges, Phys. Rev. B **80**, 064501 (2009).
[49] S. Sakai *et al.*, Phys. Rev. Lett. **111**, 107001 (2013).
[50] G. Sordi, K. Haule, and A.-M. S. Tremblay, Phys. Rev. B **84**, 075161 (2011).
[51] A. Ino, C. Kim, M. Nakamura, T. Yoshida, T. Mizokawa, A. Fujimori, Z.-X. Shen, T. Kakeshita, H. Eisaki, and S. Uchida, Phys. Rev. B **65**, 094504 (2002).
[52] A. Piriou, N. Jenkins, C. Berthod, I. Maggio-Aprile, and O. Fischer, Nat. Commun. **2**, 221 (2011).
[53] D. C. Peets, J. D. F. Mottershead, B. Wu, I. S. Elfimov, R. Liang, W. N. Hardy, D. A. Bonn, M. Raudsepp, N. J. C. Ingle, and A. Damascelli, New J. Phys. **9**, 28 (2007).
[54] Y. Ando, S. Komiya, K. Segawa, S. Ono, and Y. Kurita, Phys. Rev. Lett. **93**, 267001 (2004).
[55] O. Andersen, A. Liechtenstein, O. Jepsen, and F. Paulsen, J. Phys. Chem. Solids **56**, 1573 (1995).